

Optical trapping of colloidal particles and measurement of the defect line tension and colloidal forces in a thermotropic nematic liquid crystal

I. I. Smalyukh^{a)}

Liquid Crystal Institute, Kent State University, Kent, Ohio 44242

A. N. Kuzmin, A. V. Kachynski, and P. N. Prasad

The Institute for Lasers, Photonics, and Biophotonics, University at Buffalo, The State University of New York, Buffalo, New York 14260-3000

O. D. Lavrentovich

Chemical Physics Interdisciplinary Program and Liquid Crystal Institute, Kent State University, Kent, Ohio 44242

(Received 7 May 2004; accepted 24 November 2004; published online 5 January 2005)

We demonstrate optical trapping and manipulation of transparent microparticles suspended in a thermotropic nematic liquid crystal with low birefringence. We employ the particle manipulation to measure line tension of a topologically stable disclination line and to determine colloidal interaction of particles with perpendicular surface anchoring of the director. The three-dimensional director fields and positions of the particles manipulated by laser tweezers are visualized by fluorescence confocal polarizing microscopy. © 2005 American Institute of Physics. [DOI: 10.1063/1.1849839]

Laser tweezers,¹ in which a tightly focused beam is capable of steady trapping of small transparent particles with a refractive index higher than that of the surrounding medium, represent a valuable tool used in biology^{2,3} and physics.⁴ This optical trapping allows one to measure weak (pico-Newton) forces associated with colloidal interactions⁴ and unfolding of biomolecules.² Most of the experiments are performed in the environment of isotropic fluids, such as water. If the medium is a liquid crystal (LC), then experiments become difficult because (1) the refractive index difference between the particle and the host medium depends on the local LC director \mathbf{n} that specifies the average orientation of the LC molecules, and (2) the focused light beam can reorient the local \mathbf{n} as demonstrated for the nematic LC in flat slabs⁵ and spherical droplets.⁶ The only LC medium for which optical trapping and manipulation of colloidal particles have been successful so far, was the hyperswollen lamellar phase formed by very diluted aqueous solution of a surfactant.⁷ The nematic phase, in which one expects a wide variety of colloidal phenomena mediated by the orientational elasticity of the host medium,^{8,9} remains unstudied in this regard.

In this work, by using LCs with small birefringence and colloidal particles larger than the waist of the laser beam, we demonstrate optical trapping in the nematic thermotropic LC. We determine the trapping force, the force of elasticity mediated interaction between the pairs of particles, and also the line tension of disclinations in the nematic bulk. The three-dimensional (3D) director structures as well as the spatial positions of the particle in the LC cells are visualized using polarizing microscopy¹⁰ and fluorescence confocal polarizing microscopy (FCPM).¹¹

We used the nematic LC mixtures ZLI2806 with small birefringence $\Delta n \approx 0.04$ and average refractive index $\bar{n}_{LC} = \sqrt{(2n_o^2 + n_e^2)}/3 \approx 1.49$ ($n_o = 1.48$ and $n_e = 1.52$ are ordinary and extraordinary refractive indices, respectively) and E7 with a large birefringence $\Delta n \approx 0.23$, $\bar{n}_{LC} \approx 1.6$. Both materi-

als were obtained from EM Chemicals. The LCs were doped with 0.01 wt. % of fluorescent dye *n,n'*-bis(2,5-di-tert-butylphenyl)-3,4,9,10-perylene-dicarboximide (BTBP) for the FCPM studies.¹¹ We used melamine resin (MR) spherical particles of refractive index $n_{MR} \approx 1.68$ and diameters $D = 3$ and $4 \mu\text{m}$, and polystyrene (PS) microspheres with $n_{PS} \approx 1.6$ and $D = 1 \mu\text{m}$. The MR microspheres were tagged with the Rhodamine B dye (maximum of single-photon absorption at $\sim 540 \text{ nm}$) which fluoresced when excited by the $\lambda = 568 \text{ nm}$ Kr laser in the FCPM experiment, and also when trapped by $\lambda = 1064 \text{ nm}$ laser tweezers (the latter due to two-photon absorption). The LC containing well-separated particles (we used sonication) was introduced into thin cells of thickness $10\text{--}100 \mu\text{m}$ by capillary forces. The cells were formed by glass plates of small thickness $150 \mu\text{m}$.

We used a dual beam laser trapping system consisting of an optical manipulator (Solar-TII, LM-2), a TEM₀₀ cw Nd:YAG laser (Coherent, Compass 1064-2000) with $\lambda = 1064 \text{ nm}$, and a modified inverted microscope (Nikon, TE-200).^{3,12} An optical trap was formed by a $100\times$ microscope objective (NA=1.3) and used for 3D positioning of particles within the cell. The submicron waist size of the focused light beam ($\approx 0.8 \mu\text{m}$) is smaller than diameters of the used microspheres, which allows us to avoid reorientation of LC molecules under the intense laser radiation and its influence on the results of the measurements. The focused beam was steered in the horizontal plane by a computer-controlled galvanomirror pair; the vertical coordinate of the trap was controlled by a piezostage (accuracy $0.1 \mu\text{m}$).

Particle trapping in the nematic LC bulk. To characterize the trapping forces acting on the colloidal particles in the nematic bulk, we used the technique based on viscous drag forces exerted by the LC.¹² A laser-trapping beam rotating in the LC (frequency $\vartheta = 0.25 \text{ Hz}$) forces the particle to move around a circle of radius r . The rotation radius of r is slowly increased (increasing the particle's linear velocity) until the viscous force overcomes the trapping force and the bead escapes the optical trap along the tangential trajectory. The

^{a)}Electronic mail: smalyukh@lci.kent.edu

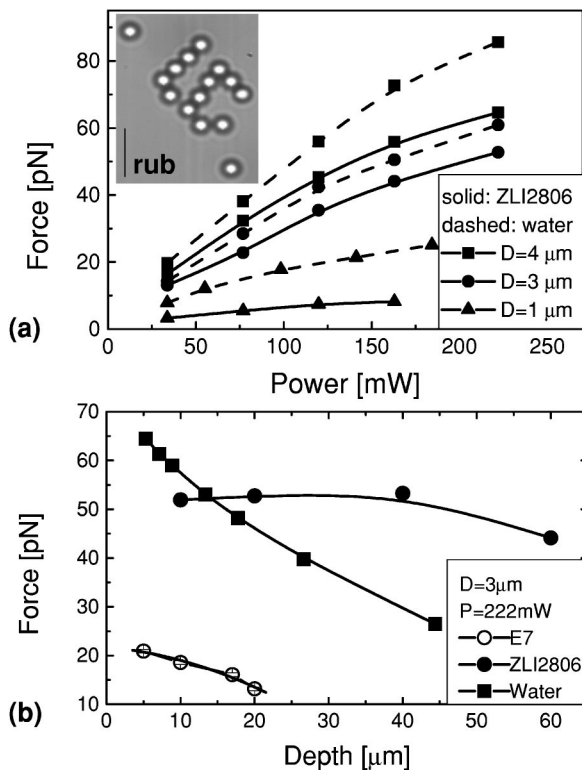


FIG. 1. Trapping force vs (a) laser power and (b) depth of trapping in liquid crystals ZLI2806 and *E7* as compared to water. The inset in (a) shows a structure of $D=3\ \mu\text{m}$ particles in form of the letters “LC” assembled in the bulk of a liquid-crystal cell; the white bar on the inset indicates the rubbing direction at the plates of the nematic cell.

trapping force F_t is calculated using the Stokes’ law $F_t \approx 6\pi^2 D \alpha_4 \partial r$. Here the effective viscosity of the LC is approximated by the Leslie coefficient α_4 .⁹ We measure the velocity of the bead at the moment of escape from the trap and thus determine F_t . The Reynolds numbers were kept low enough ($\leq 10^{-5}$) to justify the use of the Stokes’ law.^{10,12}

The optical trapping forces in LC increase with the laser power, [Fig. 1(a)]. These forces in ZLI2806 are weaker than for the same particles dispersed in water (as the difference between the refractive index of the particle and the surrounding medium is larger in the case of water) but still sufficiently strong to enable laser manipulation. The inset in Fig. 1(a) is a qualitative illustration of optical trapping of colloidal particles in the nematic bulk: the letters “LC” have been assembled by manipulating the $3\text{-}\mu\text{m}$ MR beads.

The spherical aberrations that often arise due to the refractive index mismatch at the coverslip-sample interface can weaken the trapping forces, especially if one uses oil immersion objectives for trapping particles in low-refractive index fluids such as water.¹² Because of the spherical aberrations, the spatial size of the focused light spot increases with the depth of trapping and the originally sharp intensity distribution is blurred. The spherical aberration effect on the trapping in the LC is small as the average refractive index of LCs is close to that of a silica glass, ~ 1.5 . The efficiency of trapping in ZLI2806 with a small Δn does not decrease much when the depth of scanning increases, contrary to the case of water, [Fig. 1(b)]; the particles could be trapped even at a depth of $80\ \mu\text{m}$. However, if Δn is significant, as in the case of *E7* with high $\Delta n \approx 0.23$, then substantial light defocusing weakens the trapping forces, [Fig. 1(b)]. When the trapping

depth reaches $20\ \mu\text{m}$, optical manipulation in *E7* becomes practically impossible, [Fig. 1(b)]. This result is natural, as in the birefringent media light defocusing (and the spatial dimensions of the optical trap) increases with the depth of focusing and with $|\Delta n|$.¹¹

We also observed that in the *E7* cells, the trapping forces depend on the director field along the path of light. In general, high Δn makes quantitative measurement of colloidal interaction in the standard LC such as *E7* very difficult. However, low Δn materials such as ZLI2806 are perfectly suited for optical trapping and can be used to measure colloidal interactions and parameters of topological defects in the nematic phase as we demonstrate below. Note that since the elastic constants in most nematics are $\sim 10\ \text{pN}$, the optical trap approach is ideally suited for such experiments.

Disclination line tension measurement. Topologically stable disclinations in the nematic bulk are line defects with a singular core; the director rotates by the angle π when one circumnavigates the core of the defect once¹⁰ (disclination strength $s=1/2$). Neglecting the difference in the values of Frank elastic constants, the line tension of such a disclination is approximated as¹⁰

$$T_d = \frac{\pi}{4} K \ln \frac{L}{r_c} + T_c, \quad (1)$$

where K is the average elastic constant, L is the size of the system (sample thickness in our case), r_c and T_c are the radius and energy of the defect core. In the model of an isotropic (melted) core,¹⁰ $T_c \approx \pi K/4$ and $r_c \propto 10\ \text{nm}$. With the average elastic constant for ZLI2806 $K \approx 12\ \text{pN}$ and $L = 10\text{--}100\ \mu\text{m}$, one expects, from Eq. (1), $T_d = 65\text{--}85\ \text{pN}$.

We study a straight disclination with its ends pinned at two spacers that were used to set the cell thickness, [Figs. 2(a)–2(c)]. A FCPM vertical cross section obtained with linearly polarized probing light, [Fig. 2(e)], reveals the director reorientation by π around the disclination, [Fig. 2(e)]. This configuration is assisted by the type of anchoring in the cell, which was planar at the top plate and homeotropic at the bottom plate. Both the disclination and the colloidal particle used to manipulate the line are located in the nematic bulk, [Fig. 2(f)], as one can see by colocalizing the fluorescent signals from the dye-doped LC (grayscale) and the stained particle (green). By moving the particle with the tweezers, [Figs. 2(a)–2(c)], the disclination can be pulled similarly to an elastic string. When the bead is released from the optical trap, the disclination straightens up in order to minimize its length and thus the total elastic energy, [Eq. (1)]. Displacing the particle by some distance and gradually decreasing the laser power, we find the magnitude of the pulling force F_p (equal to the optical trapping force F_t) for which $F_p = 2T_d \cos \theta_d$, where θ_d is the angle defined in Fig. 1(d). For θ_d in the range $90^\circ\text{--}45^\circ$, we find the line tension of disclination $T_d = 74 \pm 4\ \text{pN}$, close to the estimate obtained from Eq. (1) and to the data obtained by observations of thermal fluctuations of the line position.¹³

Measurement of the colloidal interaction forces in LC. We use particles with perpendicular anchoring of the director at the surface. Such a particle is equivalent to a topological radial point defect. In a cell with an overall uniform director set by the rubbing directions, the particle is accompanied by another point defect, a hyperbolic hedgehog, which guarantees the conservation of the total topological charge in the system.^{8–10,14,15} The particle—hyperbolic defect dipoles

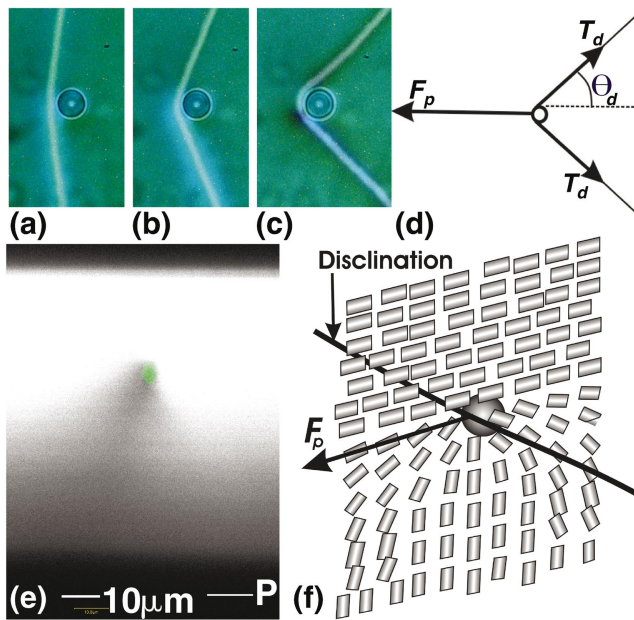


FIG. 2. (Color) Manipulation of a disclination and measurement of its line tension: (a-c) stretching the $s=1/2$ disclination in the nematic ZLI2806 with an optically trapped $D=4 \mu\text{m}$ MR bead; (d) force-line tensions balance; (e) vertical FCPM cross section with the colocalized fluorescent signal from BTBP-doped LC (grayscale) and Rhodamine B labeled particle (green); (f) schematic drawing of director field with the bead in the vicinity of a disclination. In (e) the polarization of the FCPM probing light is marked by "P" and a white bar, the BTBP dye in the LC was excited with a 488-nm Ar laser and the fluorescent light was detected in the spectral region 510-550 nm; the Rhodamine B dye incorporated in MR microspheres was excited using the 568-nm Kr laser and the respective fluorescence signal was detected in the spectral range 585-650 nm.

align parallel to the rubbing direction and form chains. For large interparticle separation distances d , when the short-range repulsion force due to the hyperbolic defect can be neglected, the attraction force along the rubbing direction has been predicted to be^{8,14}

$$F_a \approx \frac{3}{2} \pi K \alpha^2 \left(\frac{D}{d} \right)^4, \quad (2)$$

where the high-order terms in the multipole expansion are neglected, and α is a constant.

To verify Eq. (2), we studied colloidal interaction of $D=3 \mu\text{m}$ particles (MR microspheres treated with a surfactant lecithin) in ZLI2806. The uniform planar alignment in the nematic cell of thickness $\approx 40 \mu\text{m}$ (much larger than the particle size) was set by rubbing polyimide layers (PI2555) that were deposited at the inner surfaces of glass plates. Two particles are trapped in the middle of the cell, one by a fixed beam and another by a beam that can be scanned. The elastic dipoles and the separation vector between the particles are parallel¹⁵ and along the rubbing direction. For each distance d between the beads, the laser power is slowly decreased until beads escape from their traps. At the moment of escape, the measured colloidal interaction force is equal to the trapping force F_t . The attraction force as a function of particle center-to-center separation d is shown in Fig. 3. To emphasize the power-law dependence of the attraction force, we replot the force versus distance dependence in the logarithmic scale (inset of Fig. 3); the slope is 4, as expected.^{8,9,14,15} The experimental data $F_a(d)$ are fitted by Eq. (2); from the

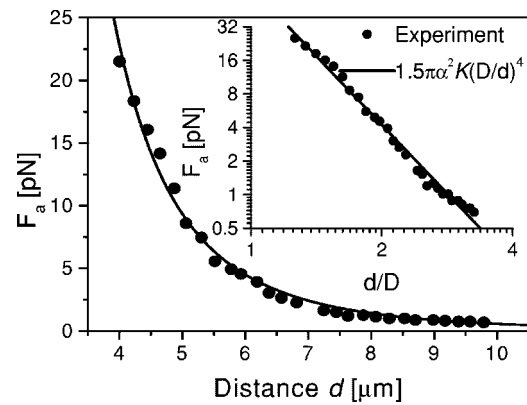


FIG. 3. Colloidal attraction force between the $D=3 \mu\text{m}$ polymer particles with perpendicular anchoring (treated with lecithin) in a planar nematic ZLI2806 cell as a function of the interparticle distance. The solid lines are the best fits to the experimental data (circles).

fitting we obtain $\alpha=1.14 \pm 0.08$. This value is smaller than the theoretically predicted $\alpha=2.04$ (calculated in the limit of infinitely strong surface anchoring)¹⁴ and somewhat larger than the value $\alpha=0.97$ obtained in Ref. 9 for ferrofluid droplets. The difference can be explained as the result of finite surface anchoring which is smaller than the one assumed in the theory¹⁴ but larger than the anchoring at the surface of ferrofluid droplets.⁹ The repulsion mediated by the hyperbolic defect is observed only at small distances, $d < 3D/2$, as expected.^{8,14,15}

In conclusion, we have used the laser tweezers to manipulate the solid particles in the nematic phase of thermotropic liquid crystals. We measured the disclination line tension and colloidal interaction forces between the particles immersed in LCs; the results are in agreement with the theoretical predictions. Laser trapping of particles in LCs opens possibilities for fundamental studies as well as for applications, such as assembling of colloidal structures and photonic crystals in the LC medium.

I.I.S. and O.D.L. acknowledge support from the NSF, under Grant No. DMR-0315523. The research at Buffalo was supported by an AFOSR DURINT grant, No. F496200110358.

¹A. Ashkin, Phys. Rev. Lett. **24**, 156 (1970).

²B. Onoa, S. Dumont, J. Liphardt, S. Smith, I. Tinoco, and C. Bustamante, Science **229**, 1892 (2003).

³P. N. Prasad, *Introduction to Biophotonics* (Wiley, New York, 2003).

⁴A. E. Larsen and D. G. Grier, Nature (London) **385**, 230 (1997).

⁵J. Hotta, K. Sasaki, and H. Masuhara, Appl. Phys. Lett. **71**, 2085 (1997).

⁶S. Juodkazis, S. Matsuo, N. Murazawa, I. Hasegawa, and H. Misawa, Appl. Phys. Lett. **82**, 4657 (2003).

⁷Y. Ivashita and H. Tanaka, Phys. Rev. Lett. **90**, 045501 (2003).

⁸Ph. Poulin, H. Stark, T. C. Lubensky, and D. A. Weitz, Science **275**, 1770 (1997).

⁹Ph. Poulin, V. Cabuil, and D. A. Weitz, Phys. Rev. Lett. **79**, 4862 (1997).

¹⁰M. Kleman and O. D. Lavrentovich, *Soft Matter Physics: An Introduction* (Springer-Verlag, New York, 2003).

¹¹I. I. Smalyukh, S. V. Shiyankovskii, and O. D. Lavrentovich, Chem. Phys. Lett. **336**, 88 (2001).

¹²A. V. Kachynski, A. N. Kuzmin, H. E. Pudavar, D. S. Kaputa, A. N. Cartwright, and P. N. Prasad, Opt. Lett. **28**, 2288 (2003).

¹³A. Mertelj and M. Čopič, Phys. Rev. E **69**, 021711 (2004).

¹⁴T. C. Lubensky, D. Pettey, N. Currier, and H. Stark, Phys. Rev. E **57**, 610 (1998).

¹⁵J. Fukuda, H. Stark, M. Yoneya, and H. Yokoyama, Phys. Rev. E **69**, 041706 (2004).